THE JOURNAL OF PHYSICAL CHEMISTRY B
A JOURNAL OF THE AMERICAN CHEMICAL SOCIETY

pubs.acs.org/JPCB

Article

Development of Imidazolium-Based Parameters for AMOEBA-IL

José Enrique Vázquez-Cervantes and G. Andrés Cisneros*

Cite This: J. Phys. Chem. B 2023, 127, 5481−5493

Read Online

ACCESS | Metrics & More | Article Recommendations | Supporting Information

ABSTRACT: A new approach for the efficient parametrization of the polarizable ionic liquid potential AMOEBA-IL and its application to develop parameters for imidazolium-based cations is presented. The new approach relies on the development of parameters for fragments that can be transferred to generate new molecules. The parametrization uses the original AMOEBA-IL parametrization approach, including the use of Gaussian electrostatic model-distributed multipoles (GEM-DM) for the permanent multipoles and approximation of the van der Waals parameters using quantum mechanics energy decomposition analysis (QM-EDA) data. Based on this, functional groups of the selected initial structures are employed as building blocks to develop parameters for new imidazolium-based cations (symmetric or asymmetric) with longer alkyl chains. The parameters obtained with this proposed method were compared with intermolecular interactions from QM references via energy decomposition analysis using symmetry adapted perturbation theory (SAPT) and counterpoise-corrected total intermolecular interactions. The validation of the new parametrized cations was carried out by running molecular dynamics simulations on a series of imidazolium-based ionic liquids with different anions to compare selected thermodynamic and transport properties, including density ρ, enthalpy of vaporization ΔH_{vap}, radial distribution function $g(r)$, and diffusion coefficients $D_{\pm}$, with experimental data. Overall, the calculated gas-phase and bulk properties show good agreement with the reference data. The new procedure provides a straightforward approach to generating the required AMOEBA-IL parameters for any imidazolium-based cation.

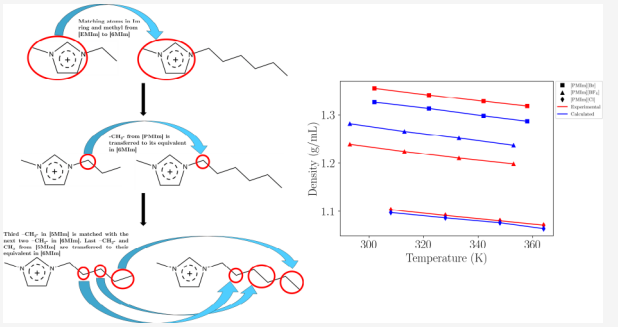

INTRODUCTION

Ionic liquids (ILs) are mixtures of cations and anions forming salts that are liquid at room temperature, remaining in that phase even at high temperatures.[1,2] The first ionic liquid was reported in 1914 by Paul Walden, synthesized by neutralization of ethylamine with concentrated nitric acid, resulting in ethylammonium nitrate salt,[3] $[EtNH_3][NO_3]$. In the 1990s, it was discovered that ILs can be stable in air and aqueous conditions, and since then, the interest in this type of systems has increased exponentially in both academia and industry.[3,4] A number of possible applications have been investigated, including (but not limited to) electrolytes for batteries, lubricants, organic solvent substitutes, biocatalysis, etc.[5−12]

The synthesis of ionic liquids can be carried out by combining a (generally) asymmetric organic cation with an inorganic anion.[3] This means that, having a single cation, it is possible to combine it with one of the numerous anions available, forming a different ionic liquid with each combination. One of the most investigated cations is imidazolium $[Im^+]$ due to its particular properties such as the ease with which the alkyl chain length can be modified on the nitrogen atoms of the $[Im^+]$ ring, being an interesting option to develop more solvents by combining it with different anions, using the same basic structure for the cation.[1] The versatility of $[Im^+]$ cation is one of the reasons why $[Im^+]$-based ILs are some of the most employed ILs in industrial applications.[13]

The vast possibilities for synthesizing ionic liquid pairs result in the quandary of determining these compounds' properties at a reasonable time and cost. Computer simulations have become a useful tool in studying and determining the properties of ionic liquids as well as predicting specific ionic liquids with desired properties.[14,15] Molecular dynamics (MD) simulations to investigate ILs[16,17] can be carried out using nonpolarizable[18] or polarizable[19] force fields. The latter option provides an approach that explicitly includes the electronic polarization contribution, which may play an important part in these systems.[20]

We have developed an all-atom polarizable IL potential based on the AMOEBA force field, termed AMOEBA-IL.[14,21] AMOEBA-IL uses distributed multipoles obtained from the Gaussian electrostatic model (GEM-DM).[22,23] GEM-DM has been shown to be transferable for the development of atom-

Received: February 13, 2023
Revised: May 22, 2023
Published: June 8, 2023

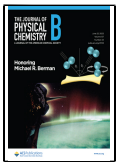

centered multipoles for the AMOEBA force field.[24] So far, AMOEBA-IL has been limited to a small number of cations and anions due to the costly parametrization procedure, which involves the determination of distributed multipoles for each molecule. We have shown that AMOEBA-IL can accurately reproduce bulk properties.[14,21] Additionally, AMOEBA-IL has been shown to predict properties for previously uncharacterized pairs. Specifically, for spirocyclic pyrrolidinium [$sPyr^+$] and [BF_4^-], calculations with AMOEBA-IL prior to the experimental synthesis of the ions predicted the melting point for this ion pair within 2% of the subsequently calculated value.[15]

In this contribution, we present a new method for the parametrization of imidazolium-based AMOEBA-IL cations consisting of transferring the parameters of specific fragments of previously parametrized groups of the alkyl chain of a relatively small imidazolium cation to form new cations by just adding specific parametrized functional groups in asymmetric imidazolium-based cations, referred as initial structures (imidazolium ring, methyls, and methylenes), from 1-ethyl-3-methylimidazolium, [EMIm], 1-propyl-3-methylimidazolium, [PMIm], 1-butyl-3-methylimidazolium, [BMIm], and parametrized groups of symmetric imidazolium-based cations from 1,3-diethylimidazolium, [diEIm], and 1,3-dibutylimidazolium, [diBIm], to imidazolium-based cations with longer alkyl chain (Figure 1). The new procedure is tested by generating

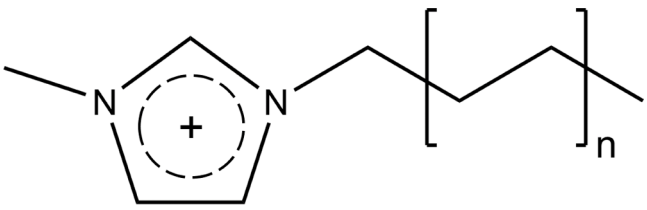

Figure 1. General structure of imidazolium-based cations derived in this work.

parameters for medium- and long-chain symmetric such as 1,3-dihexylimidazolium, [di6Im], and asymmetric imidazolium-based cations such as 1-pentyl-3-methylimidazolium, [5MIm], 1-hexyl-3-methylimidazolium, [6MIm], 1-hexyl-3-ethylimidazolium, [6EIm], and 1-dodecyl-3-methylimidazolium, [12MIm] (see Supporting Information). MD simulations were performed to calculate various bulk properties. Our results show that the transferred parameters show minimal loss of accuracy compared with the full parametrization procedure, and good accuracy in comparing calculated bulk properties with experimental data.

The remainder of the paper is as follows: in the next section we describe the details of the previous parametrization approach, the new method to transfer the required parameters to generate arbitrary alkyl chains in imidazolium cations, and details of the MD simulations and analyses. Subsequently, results for gas-phase and bulk calculations are presented and compared with reference data from the literature for selected imidazolium-based IL combinations, followed by concluding remarks.

COMPUTATIONAL METHODS

Parametrization of Imidazolium-Based Cations for AMOEBA-IL. The parametrization procedure for the starting structures follows the AMOEBA modified parametrization method reported previously.[14] Briefly, the AMOEBA potential[25−27] includes bonded and nonbonded terms to reproduce inter- and intramolecular interactions.

$$V = V_{bond} + V_{angle} + V_{b\theta} + V_{out} + V_{torsion} + V_{Coul} + V_{Pol} + V_{vdW} \quad (1)$$

where V_{bond}, V_{angle}, $V_{b\theta}$, V_{out}, and $V_{torsion}$ are bond stretching, angle bending, bond-angle cross term, out-of-plane bending, and torsional rotation modes, respectively. The remaining terms, V_{Coul}, V_{Pol}, and V_{vdW} correspond to the nonbonded intermolecular interactions: Coulomb, polarization, and van der Waals, respectively.

AMOEBA is a polarizable force field that uses a multipole expansion up to quadrupoles on specific centers (atoms) to represent the permanent electrostatic component. The polarization is taken into account using the induced atomic dipoles approach[20] coupled with a Tholé damping function to avoid the so-called "polarization catastrophe" at short distances.[27]

For van der Waals interactions, the buffered Halgren pairwise potential is employed following the AMOEBA FF functional form.[28] The mathematical form of this potential is as follows:

$$V_{vdW}(r_{ij}) = \varepsilon_{ij}\left(\frac{1+0.07}{\left(\frac{r_{ij}}{R_{ij}^0}\right)+0.07}\right)^{14-7}\left(\frac{1+0.12}{\left(\frac{r_{ij}}{R_{ij}^0}\right)^7+0.12}-2\right) \quad (2)$$

where ε_{ij} is the potential well, r_{ij} is the separation distance between sites i and j, and R_{ij}^0 is the minimum energy interaction distance for sites i and j.

AMOEBA-IL follows the AMOEBA procedure to parametrize the bonded terms.[29] The nonbonded terms are initially parametrized by comparing individual intermolecular interaction contributions of gas-phase dimers to QM energy decomposition analysis (QM-EDA) reference values as described in ref 14. In the current work, we have used DFT-based symmetry adapted perturbation theory (SAPT-DFT) to obtain the reference QM intermolecular interactions.[30] Once the initial nonbonded terms are parametrized, bulk simulations are carried out to calculate densities and heats of vaporization to determine the accuracy of the parameters and, if needed, adjust the Halgren parameters to optimize agreement for both gas-phase and bulk properties.[15,31,32]

As mentioned above, the distributed multipoles are obtained by using GEM-DM. The procedure to obtain GEM-DM has been discussed in detail previously in refs 23, 24, and 33. Briefly, GEM-DM multipoles are extracted from fitted GEM densities directly. The GEM densities are fitted by minimizing the error of the intermolecular Coulomb interaction for a series of dimers, here composed of the initial [Im^+]-based cation structures and an already parametrized water molecule[34] as a function of the distance between the monomers (cation position fixed) on the same axis with increments of 0.5 Å from one dimer to the next one.[14,34] The intermolecular Coulomb interaction reference values were obtained using the symmetry-adapted perturbation theory (SAPT) method implemented in Psi4.[30] Validation for the calculated total energies of the parametrized fragments was done by comparing counterpoise corrected total intermolecular interactions computed with Gaussian 16 package[35] at the MP2(full)/aug-cc-PVTZ level of

https://doi.org/10.1021/acs.jpcb.3c00986
J. Phys. Chem. B 2023, 127, 5481−5493

theory. Additionally, the total intermolecular interaction at the second-order perturbation was calculated with SAPT as implemented in Psi4. On the other hand, the Coulomb and total intermolecular energies reproduced by the developed parameters were calculated with the *analyze* program of TINKER.[36]

Comparison between Structure Minimization with GEM-DM and QM Geometry Optimization. In order to test the accuracy of the intra- and intermolecular interactions for a single cation, a geometry optimization of a distorted [5MIm] was computed using both TINKER and Gaussian 16. A geometry optimization using AMOEBA-IL was performed with the minimization routine implemented in TINKER 8.7. Geometry optimization of the distorted [5MIm] in Gaussian was calculated at the MP2/cc-PVTZ level of theory. Root mean squared deviation (RMSD) calculation of the overlapped structures was performed in VMD for quantitative and qualitative analysis of the optimized structures.

Parameter Transfer for AMOEBA-IL Imidazolium Cations. The parametrization procedure described above requires that each individual cation is parametrized separately. However, given the vast diversity of symmetric and asymmetric cations, we wanted to investigate the possibility of transferring parameters of specific molecular fragments from previously parametrized imidazolium-based cations.

To this end, the [Im$^+$]-based cations considered as starting structures for the reference parametrization were [EMIm], [diEIm], [PMIm], [BMIm], and [diBIm]. Once the parameters for all the initial structures were obtained and tested, the imidazolium and methyl group from the [EMIm] were taken as one of the functional groups used to construct new cations. The parameters for the remaining [Im$^+$]-based cations were transferred from functional groups of selected [Im$^+$]-based cations parametrized with the original method.

The methylenes and methyl groups from alkyl chains in each of the starting structures were analyzed to compare the differences in individual multipolar components between each considered fragment (van der Waals parameters remained the same). The analysis of all the functional groups showed that the multipoles from [diEIm] were very different from the rest of the cations. The ethyl groups on both sides of [diEIm] presented different charges than the corresponding ethyl group in [EMIm]. Additionally, having methylenes bonded to the nitrogens in [diEIm] makes these groups chemically different from methylenes placed further away from the ring along the alkyl chain. This indicated that the ethyl groups in [diEIm] would not be amenable as an initial structure for asymmetric or symmetric cations, and thus [diEIm] parameters were deemed to be not transferable from the starting structures (see Supporting Information).

To form the basic structure of an asymmetric cation with a *n*-carbon alkyl chain, the methylene group bonded to its corresponding nitrogen in the ring was taken from [PMIm], parametrized in this work following the standard procedure (see above). For the rest of the methylenes in the *n*-carbon alkyl chain, the multipoles were taken directly from [BMIm], also parametrized in this work, following the original procedure. The same idea was applied to symmetric cations. The basic structure for this type of cations is [diBIm], and its basic structure was tested by transferring parameters to similar symmetric cations with longer alkyl chains, for example, [di6Im].

In molecules with conformational flexibility, it has been shown the dependency of the electrostatics on the conformation of the molecule and how defining polarizable groups within the same molecule improves the polarizable force field description of possible conformers.[25] To account for internal polarization, in each of the starting structures, the methyl group bonded to its corresponding nitrogen, the imidazolium ring, each methylene, and the methyl of the alkyl chain were considered as individual polarization groups. This means that the number of polarizable groups in a specific cation depends on the number of carbons contained in each alkyl chain. Figure 2 shows the imidazolium-based cations taken as starting

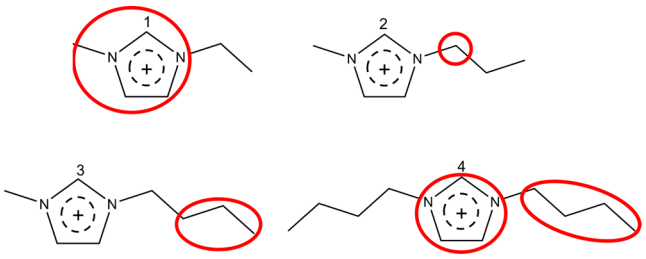

Figure 2. [Im$^+$]-based cations used as initial structures to build new [Im$^+$]-based cations: (1) 1-ethyl-3-methylimidazolium, (2) 1-propyl-3-methylimidazolium, (3) 1-butyl-3-methylimidazolium, and (4) 1,3-dibutylimidazolium. Functional groups from each starting molecule used to form new cations are enclosed in red.

structures for the rest of the cations built with the proposed approach. Figure 3 shows a schematic representation of the parametrization of 1-hexyl-3-methylimidazolium [6MIm] from the existing parameters.

MD Simulation Details. Molecular dynamics (MD) simulations for cubic cells including 200 ionic pairs were performed with the AMOEBA-IL force field using the GPU version of TINKER 8.7, following a stepwise procedure for heating the system to the target temperature (the temperature with available experimental data for comparison). For each temperature, 1 ns *NPT* simulations with an integration step of 1 fs, nonbonded cutoff of 10 Å, and sampling each 10 ps were performed. For the heating process, the RESPA integrator, Bussi thermostat, and Berendsen barostat were employed. Long-range electrostatic effects were calculated via the smooth particle mesh Ewald (sPME) method, with a 10 Å real-space cutoff.[37,38] The dimensions for the sPME reciprocal space grid were set as the closest integer to 1.2 times the axis of the cubic cell. Isotropic long-range corrections for the van der Waals term were used to account for van der Waals interactions beyond a cutoff distance of 10 Å.[39] Test calculations with van der Waals cutoffs of 8 and 14 Å were performed to determine the influence of the cutoff. The values of the calculated properties did not change compared to the original 10 Å cutoff (results not shown).

After equilibration, the systems were subjected to 10 ns of MD in the *NPT* ensemble. In all cases, the RESPA integrator, Bussi thermostat, and Montecarlo barostat were used for all IL systems studied. The integration step used was 1 fs, and sampling was done each 1 ps. A nonbonded interaction cutoff distance of 10 Å was used, coupled with PME. PME summation was set as the closest integer to 1.2 times the axis of the cubic cell.

All the imidazolium-based IL combinations studied in this work are condensed in Table 1. In total, simulations for 17

https://doi.org/10.1021/acs.jpcb.3c00986
J. Phys. Chem. B 2023, 127, 5481−5493

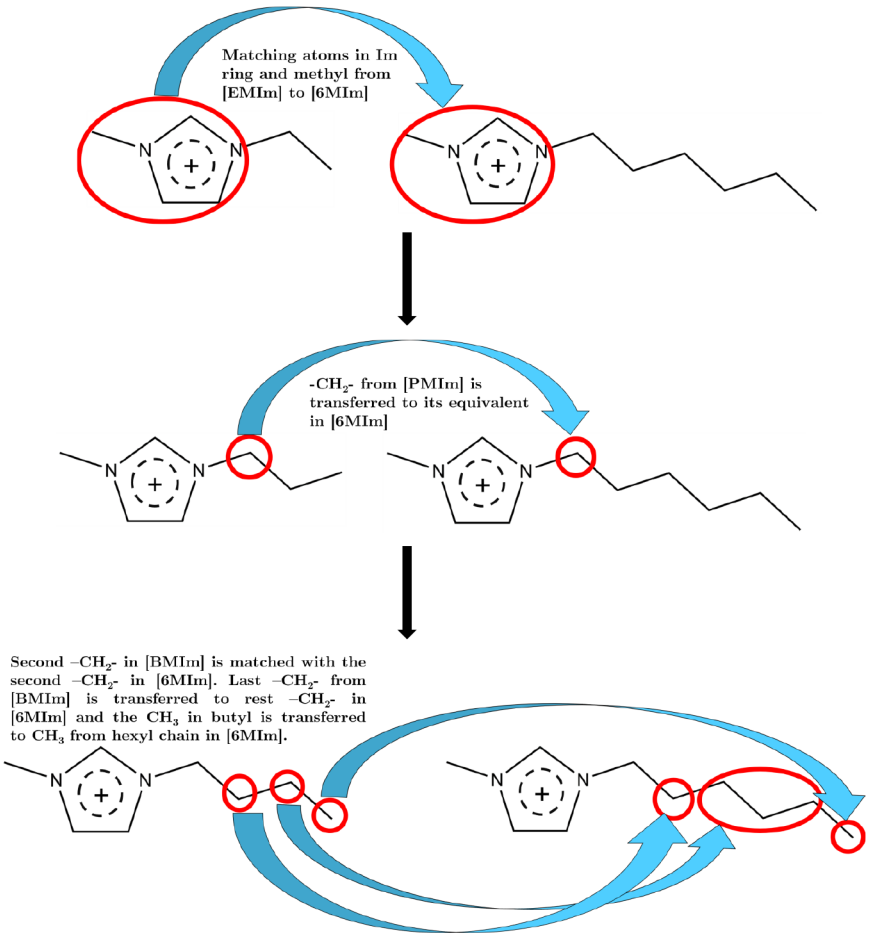

Figure 3. Example of how [6MIm] was developed from initial structures using the proposed method.

Table 1. List of IL Pairs Studied in This Work[a]

	anion				
cation	[Cl]	[Br]	[NO_3]	[BF_4]	[$EtSO_4$]
[diEIm]	√	√	-	√	√
[PMIm]	√	√	√	√	-
[EMIm]	-	-	-	√	-
[BMIm]	-	√	-	√	-
[5MIm]	-	√	-	-	-
[6MIm]	√	-	-	-	-
[diBIm]	-	√	-	-	-
[di6Im]	-	√	-	-	-
[6EIm]	-	√	-	-	-
[12MIm]	√	-	-	-	-

[a]Cations in italics were parametrized with the original method. Cations derived from the proposed method are denoted in bold.

distinct IL combinations have been performed at three different temperatures. All anions used in this work were parametrized previously. Results for [EMIm], [PMIm], [BMIm], [5MIm], [diBMIm] [6MIm], and [6EIm] based ILs are discussed below. The remaining cations with their respective anion pairs are included in the Supporting Information.

The quality of the parameters for the initial molecules and the cations built from them was tested by calculating gas-phase and selected bulk properties including density (ρ) and enthalpy of vaporization (ΔH_{vap}) at selected temperatures. The latter property was calculated following the procedure described in ref 27, where the enthalpy of vaporization is expressed as the difference in the potential energy (E_{pot}) between the gas and liquid phase.

$$\Delta H_{vap} = E_{pot}(\text{gas}) - E_{pot}(liq) + RT \tag{3}$$

with the potential energy of the gas phase calculated by running stochastic molecular dynamic simulations on an isolated ionic pair at the desired temperature in TINKER.

Self-diffusion coefficients are another liquid property that provides evidence of the robustness of the force fields used in MD simulations. This property depends on many parameters such as geometric structure, ion size, charge delocalization, and strength of intermolecular interactions. The diffusion coefficients were obtained via the diffuse routine in TINKER, which uses Einstein's relation

$$D_{\pm} = \lim_{t\to\infty} \frac{\langle \text{MSD}(t)_{\pm} \rangle}{6t} \tag{4}$$

Site−site radial distribution function ($g(r)$) was calculated in order to get insights about the interionic correlations of the ILs. The $g(r)$ can be easily computed from production trajectories using VMD.[40] Finally, spatial distribution function (SDF) was computed with TRAVIS[41,42] to study the type of interaction between the carbon atoms of the imidazolium ring from the cation and the anion.

Cation self-diffusion coefficients were calculated from the production trajectories as the mean square displacement

https://doi.org/10.1021/acs.jpcb.3c00986
J. Phys. Chem. B 2023, 127, 5481−5493

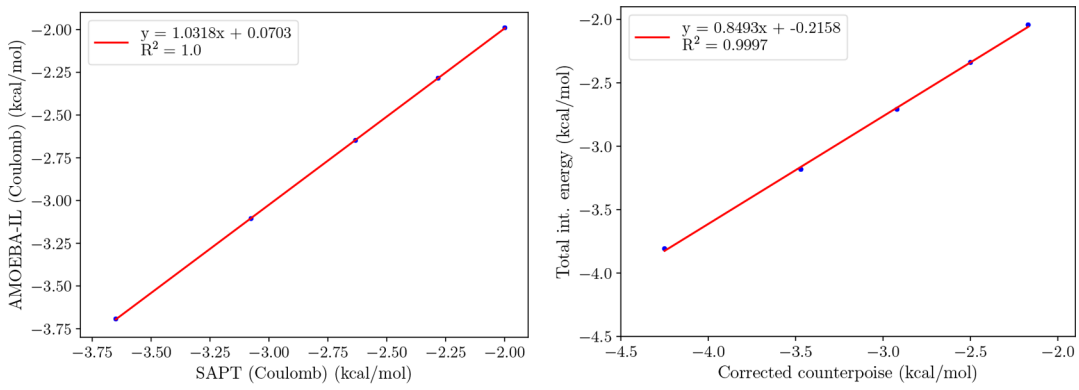

Figure 4. (a) AMOEBA-IL Coulomb with multipoles from GEM-DM was fitted with respect to SAPT reference for 5 [PMIm][H_2O] dimers. (b) Total intermolecular energy comparison for the same dimers.

⟨MSD(t)⟩ at the center of mass of the molecule. To ensure that all the systems studied reached the diffusive regime, the slope of the MSD log−log plot was calculated for each system using the last 5 ns of simulation.[43] In all cases, a slope of 1 was obtained (examples shown in Figure S2). Box-size effects corrections have been included using the procedure reported by Yeh and Hummer.[44]

RESULTS AND DISCUSSION

Parametrization and Transferability. The parametrization was performed in the initial structures except [EMIm] because this cation was previously reported.[31] A reference water molecule[34] was used to form a set of dimers with [PMIm], [BMIm], and [diBIm]. The Coulomb term was computed with GEM and GEM-DM for all dimers and compared with the electrostatic term obtained from SAPT.

Figure 4 shows a comparison of the Coulomb and total intermolecular interaction energies calculated with AMOEBA-IL and SAPT for 1-propyl-3-methylimidazolium interacting with a water molecule in five random orientations. Similar comparisons for other cations parametrized with the original procedure, [5MIm], and the new method, [6MIm], are shown in Figures S1 and S2. In all cases good agreement between the AMOEBA-IL parameters and SAPT is obtained.

Single Molecule Conformational Analyses. We performed several calculations to test the performance of the parameters for a single cation. A distorted structure for the [5MIm] cation was generated where the ring was elongated by 30% along the N1 atom, and two methylene units were also distorted (see Supporting Information). The geometry of this structure was optimized with Gaussian 16 and TINKER to compare the final minimized coordinates.

Figure 5 shows the superposition of the optimized structures with both TINKER and Gaussian. The final root mean squared deviation (RMSD) for both structures is 0.16 Å, which shows the calculated parameters are able to reproduce intramolecular structural properties.

An analysis of six conformers was done for the [5MIm] cation. Single point (SP) calculations for six different (labeled C1, C2, ..., C6) conformations of [5MIm] were performed with Gaussian 16 at the ωB97XD/cc-PVTZ level of theory. Total potential energies of the same six conformers (labeled the same as QM the reference) were calculated using the AMOEBA-IL parameters. Figure 6a shows the energies of the different conformers (Figure 6b) relative to the lowest energy conformer.

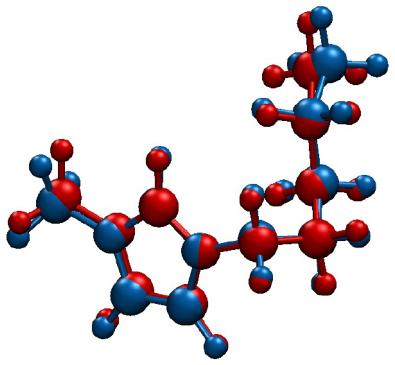

Figure 5. Structural comparison of [5MIm] optimized with AMOEBA-IL (red) and Gaussian 16 (blue) starting from a distorted structure.

A similar analysis was performed for a series of 10 conformers of [di6Im] cation to investigate the larger conformational space allowed by the two alkyl chains. Figure 7a shows the plot of [di6Im] with the relative energies of the studied conformers (Figure 7b). In the case of both cations, it can be observed that AMOEBA-IL total energies follow the same trend as the QM reference with very few exceptions. Deviations concerning the absolute energies are observed, in particular for conformers where the chains are oriented closer to the ring (Figure 7a).

The observed energy deviations for these conformers may be attributed to several factors such as errors from the bonded energy terms or penetration effects between the tails of the alkyl chains and the ring or methylene carbons closer to the rings.

Radial Distribution Functions (RDFs). Site−site radial distribution function $g(r)$ out to a 20 Å radius was calculated for all the systems studied at different temperatures, depending on the availability of previously reported data. It was also possible to compare site−site $g(r)$ of systems where the size of the cation was similar to the cation with reported data. Figure 8a shows the calculated $g(r)$ in this work for [EMIm][BF_4], where the hydrogens used as reference sites for the cation are marked in red, and the sites of the anion used for this calculations were the fluorine atoms.

https://doi.org/10.1021/acs.jpcb.3c00986
J. Phys. Chem. B 2023, 127, 5481−5493

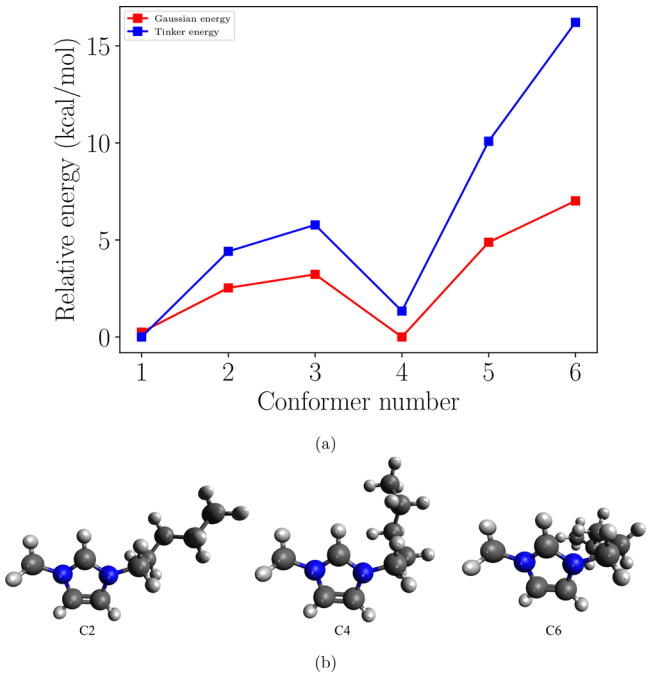

Figure 6. (a) Energy of six different conformers of [5MIm]. Labels indicate the same conformers in Gaussian and TINKER. (b) Examples of some of the [5MIm] conformers used for comparison.

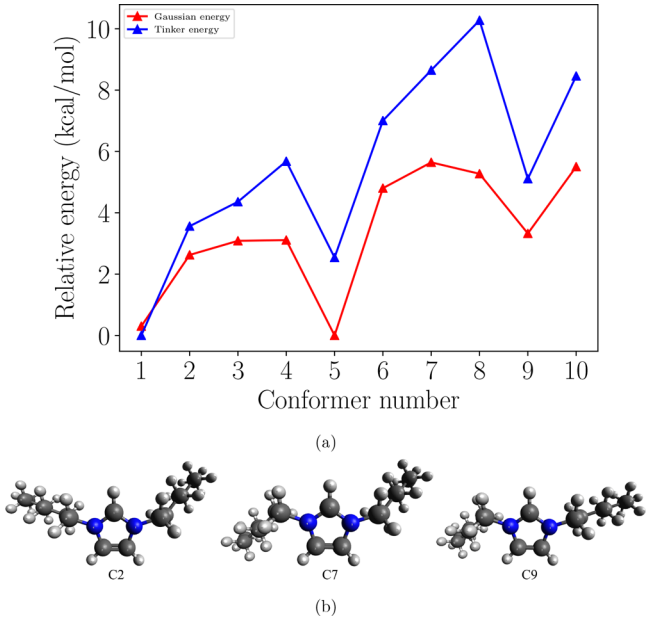

Figure 7. (a) Energy of 10 different conformers of [di6Im]. The labeling is the same as in the case of [5MIm]; e.g., the geometry of C2 is the same in both calculations, Gaussian and TINKER. (b) Examples of some of the [di6Im] conformers used for comparison.

Small differences are observed with respect to previously reported data given that atoms H4 and H5 in [EMIm] were considered equivalent for their respective parametrization procedure[31] and included in AMOEBA-IL. Overall, the calculated site−site $g(r)$ presents a pronounced peak at 2.5 Å and another small peak at 5 Å as reported elsewhere.[45] In general, the patterns found in the calculated $g(r)$ are in agreement with related RDFs reported previously using computational studies for this IL at the same temperature.[45] The small shoulder at 10 Å is more pronounced in the calculated $g(r)$ in this work probably because of the equivalence of atoms H4 and H5.

Calculated RDFs for [PMIm][Cl] were compared to the data reported for the [EMIm][Cl] system.[45] Since [PMIm] is just one carbon longer than [EMIm], it is reasonable to assume that similar patterns may be observed when the same anion is used. Figure 8b shows the sites from [PMIm]; in this case, all marked atoms were considered different atoms in AMOEBA-IL for this work. For [PMIm][Cl], similar peaks for H2, H4, and H5 are found compared with the computed reference.[45] A more intense peak at 2.5 Å is observed for the three sites computed in the cation with respect to the [Cl]. The shoulder at 6.5 Å is more pronounced in [PMIm][Cl] due probably to stronger attractive Coulomb interactions with the anion as noticed for the parametrized cations in this work. These calculations provide evidence of expected behavior for ILs similar to a previously calculated reference.

Figure 8c shows $g(r)$ for [5MIm][Br] as a prediction for this system because neither experimental nor computational data have been reported. In this case, marked in red are the sites for [5MIm], in which all the hydrogen atoms selected were defined as different atoms in AMOEBA-IL. A peak is observed around 3 Å for the sites selected. There are two more peaks between 5 and 7 Å due to the interactions of H4 and H2 with [Cl], respectively. The pattern for this IL is very similar to the one observed for [PMIm][Cl] 8b.

Spatial Distribution Function (SDF). Spatial distribution function (SDF) analyses for [5MIm][Br] and [6MIm][Cl] were computed to compare the distribution for an IL pair where the cation was fitted with the original procedure and one with a cation for which the parameters were obtained with the transfer procedure. In both cases, the distribution is calculated with respect to the carbons of the imidazolium ring and the corresponding anion.

Figure 9 shows that large surfaces are observed opposite to the carbon atoms of the imidazolium (Im) ring. This is consistent with the fact that hydrogen atoms in aromatic systems tend to be more electrophilic in resonant systems. The longer alkyl chain bound to C3 can orient toward one face of the ring resulting in preferential interaction of the anion with the opposite face. These results are in agreement with the observations for the aromatic hydrogens in the RDF calculations (see Figure 8).

Densities. Densities for [Im$^+$]-based cations parametrized with the original procedure and with the transferred approach were calculated at three different temperatures and compared with their respective available experimental data. For the [EMIm][BF_4] combination, previously reported parameters were used.[14,31] Figure 10a shows that the calculated density for [EMIm][BF_4] at three different temperatures is in good agreement with available experimental data.[46,47] The computed densities at 293, 328, and 353 K were 1.270 g/cm^3, 1.308 g/cm^3, and 1.288 g/cm^3, respectively, compared with their experimental counterparts of 1.286 g/cm^3, 1.265 g/cm^3, and 1.253 g/cm^3 at the same temperatures.

The [EMIm] was defined to have three polarization groups given the importance of internal polarization in ILs as discussed by Torabifard et al.[15]

The error between the calculated and experimental data is less than 4% for each temperature. The van der Waals parameters for [EMIm] were adjusted to fit better with experimental ΔH_{vap} (discussed below). It is possible that the

https://doi.org/10.1021/acs.jpcb.3c00986
J. Phys. Chem. B 2023, 127, 5481−5493

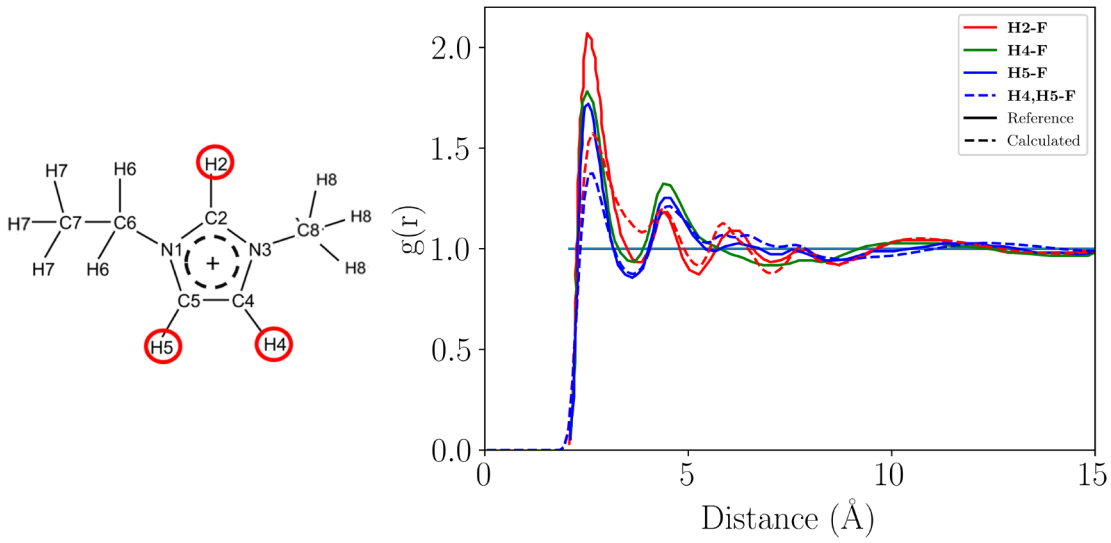

(a) Calculated site-site RDF for [EMIm][BF_4] IL at 380 K.

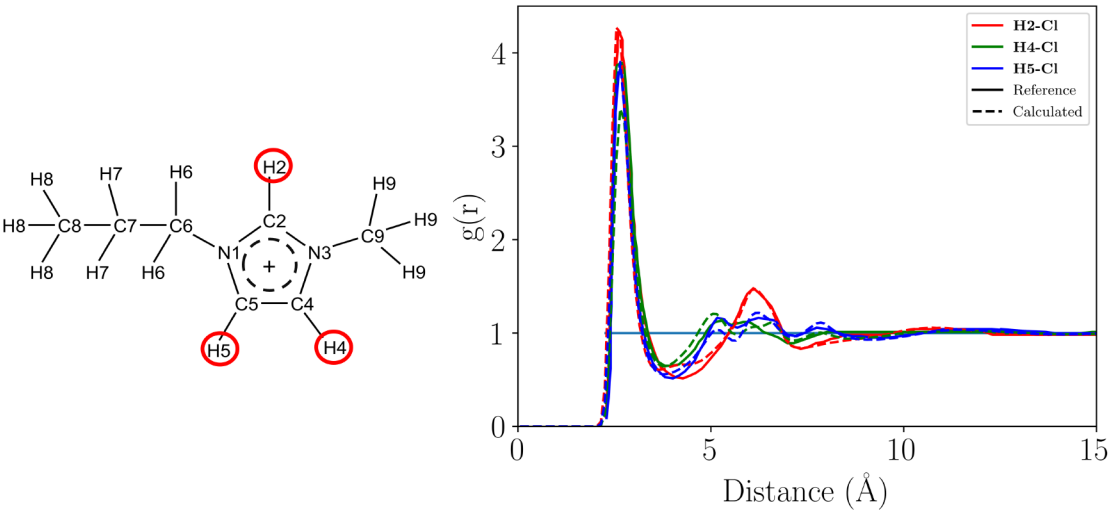

(b) Calculated site-site RDF for [PMIm][Cl] at 390 K compared with [EMIm][Cl] from the reference.

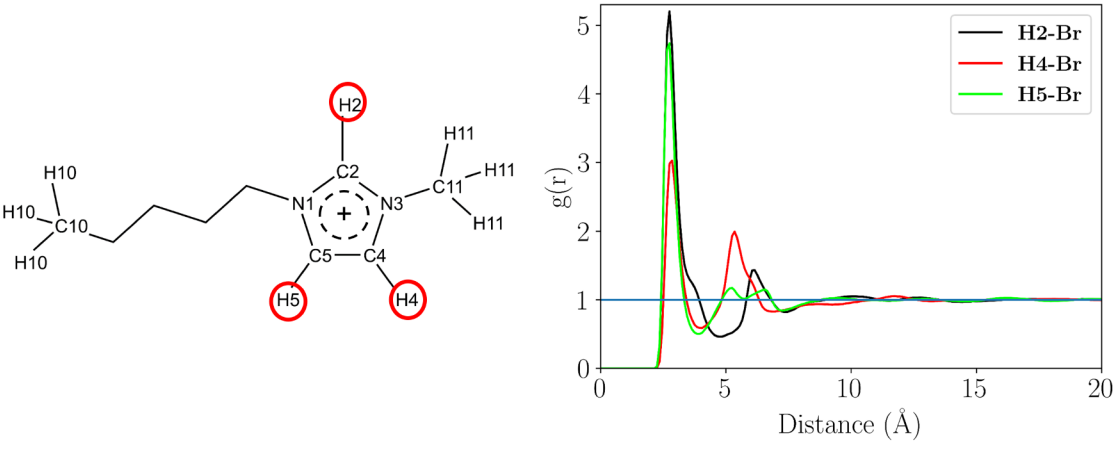

(c) Calculated site-site RDF for [5MIm][Br] IL at 303 K.

Figure 8. Radial distribution functions for selected ILs.

parameters used for van der Waals resulted in slightly more attractive interactions at lower temperatures, but this attraction is relatively compensated at higher temperatures.

Parameters for the [PMIm] cation were determined using the original parametrization as described in the methods section. Due to the amount of available experimental data, it

https://doi.org/10.1021/acs.jpcb.3c00986
J. Phys. Chem. B 2023, 127, 5481−5493

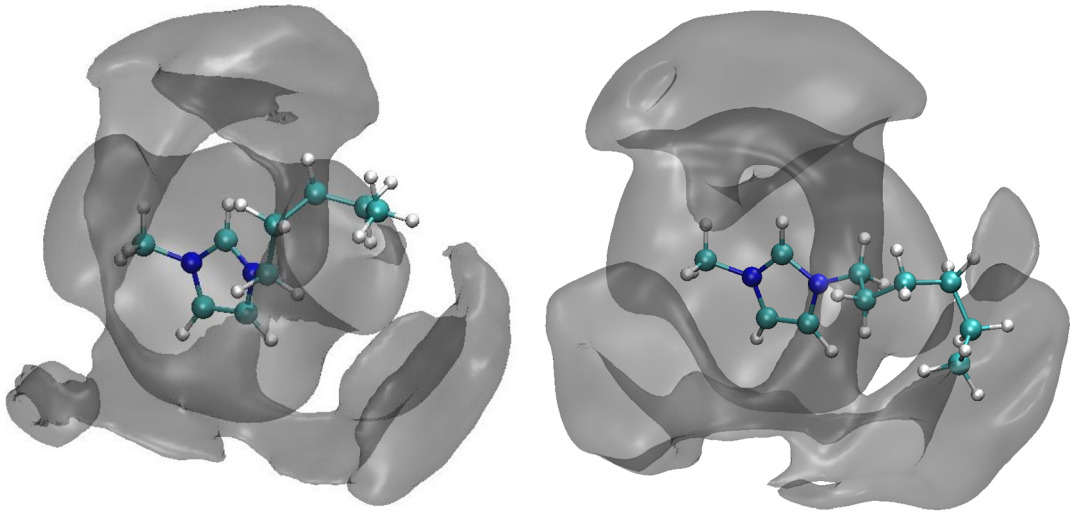

(a) [5MIm][Br]. (b) [6MIm][Cl].

Figure 9. (a) Calculated structure distribution function (SDF) for [5MIm][Br], (b) SDF for [6MIm][Cl], isovalue = 0.5 and maximum observation radius = 10 Å. The plots show the distribution of the anions around the cation.

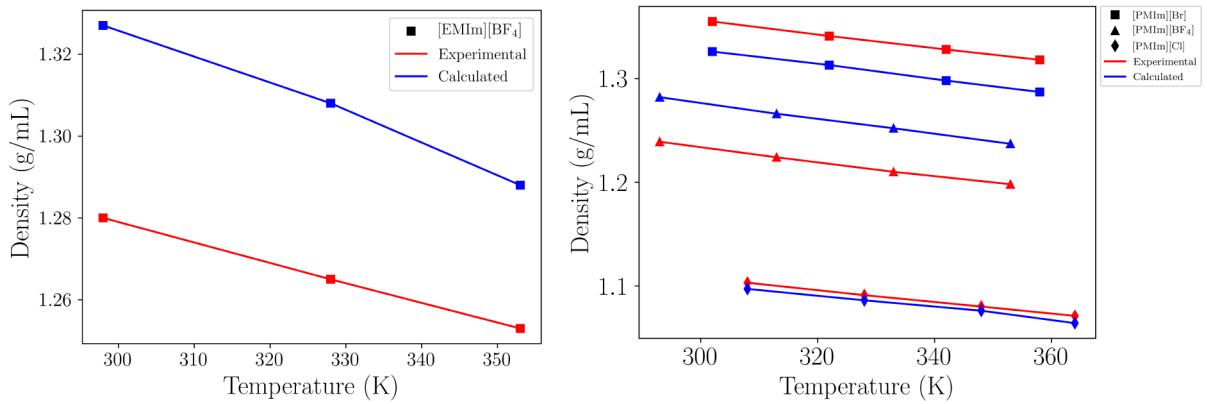

(a) (b)

Figure 10. (a) Calculated and experimental densities for [EMIm][BF_4]. (b) Calculated and experimental densities for [PMIm]-based ionic liquids at different temperatures. [EMIm] and [PMIm] cations are starting structures, and their parameters were obtained following the original method.

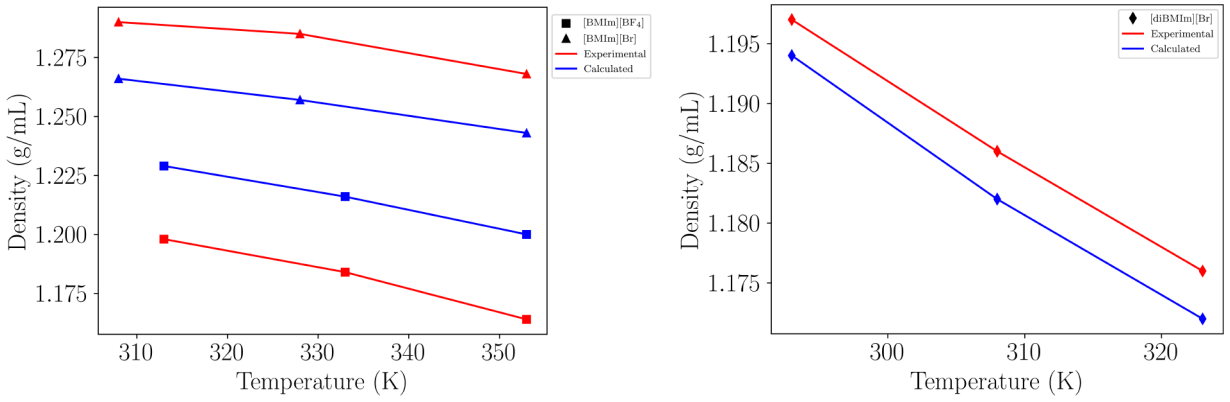

(a) (b)

Figure 11. (a) Comparison of calculated densities of [BMIm]-based ILs with experimental data. (b) Comparison of calculated densities of [diBIm]-based ILs with experimental data. [BMIm] and [diBIm] cations are starting structures, and their parameters were obtained following the original method.

https://doi.org/10.1021/acs.jpcb.3c00986
J. Phys. Chem. B 2023, 127, 5481−5493

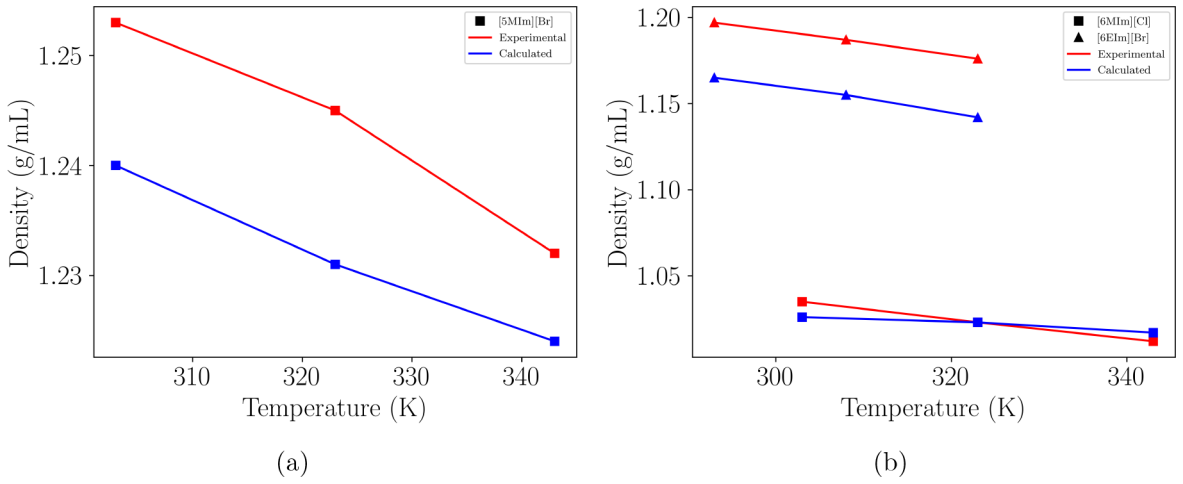

Figure 12. (a) Calculated densities comparison of [5MIm]-based ILs with experimental data. (b) Calculated densities for [6MIm]-based and [6EIm]-based ILs compared with experimental data. [5MIm], [6MIm], and [6EIm] were constructed using the proposed method in this work to transfer parameters from small [Im^+]-based cations to bigger cations of the same family.

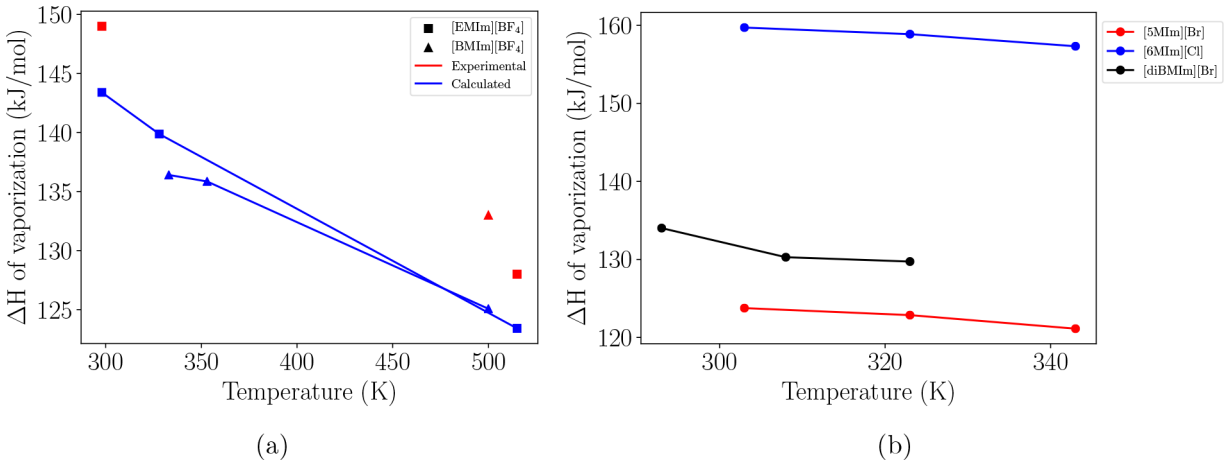

Figure 13. (a) Comparison of calculated and experimental enthalpy of vaporization of ILs with available experimental data. (b) Calculated enthalpy of vaporization of ILs without available experimental data.

was tested to form as many ILs as possible with the anions available in the AMOEBA-IL anion parameter set.[14] Figure 10b shows the [PMIm]-based ILs calculated compared with their respective experimental densities.

When compared with experimental data, the calculated density values for [PMIm][Br],[48] [PMIm][BF_4],[49,50] and [PMIm][Cl],[51] show good agreement. Additionally, a relation between the size and shape of the anion and the accuracy of the calculations begins to emerge. The smaller the anion, the higher is the accuracy. This can be reasonable because one-atom ions just have the monopole term (charge) to be reproduced by the force field. On the other hand, the relatively small size of [PMIm] implies fewer possible degrees of freedom for the propyl chain and the number of possible interactions with the bromine cations is reasonably small.

For [BMIm][BF_4],[52,53] an overestimation of the density is observed, which is consistent with the observation on [EMIm][BF_4] (Figure 11a). This indicates that the parameters result in a slightly more attractive interaction between the cations and the anions.

The experimental densities for [BMIm][Br][54,55] are higher compared with the calculated one. This is likely due to shortcomings in the [Br] parameters. In this particular case, the vdW parameters for [Br] had to be modified to fit better with the ΔH_{vap} (explained below).

For [5MIm][Br], the calculated densities and the experimental references[54,56] show similar trends. The error is systematically consistent within 5%. On the other hand, for [diBIm][Br], the trend and densities fit better with the experimental reference[1] (Figure 11b). The increased accuracy for the bulk properties may be due to the symmetry of the cation, which exhibits a more evenly distributed electronic charge density around the molecule.

Densities for parametrized [Im^+]-based ILs using the transferred method are shown in Figure 12 and in Supporting Information. [5MIm], [6MIm]-based, and [6EIm]-based ILs show good agreement with experimental data. The parameters for their imidazolium ring and the methyl group were taken from [EMIm]. The pentyl and hexyl groups were constructed using the equivalent atoms from the butyl group in [BMIm], as described in previous sections.

In all [Im^+]-based ILs parametrized using the transferred procedure, errors within 5% are observed compared with the experimental data, and the calculated densities show a similar slope with respect to the experimental one as temperature increases.

https://doi.org/10.1021/acs.jpcb.3c00986
J. Phys. Chem. B 2023, 127, 5481−5493

This suggests that the transferability of multipole parameters for the selected fragments to similar molecules results in an accurate description of the new [Im$^+$]-based cation.

For [5MIm][Br], the calculated densities and the experimental references[54,56] show similar trends. The error is systematically consistent within 5%. It is observed that the accuracy of the proposed model is acceptable under the established criteria in this work (≲5%). The experimental densities for [BMIm][Br][54,55] are higher compared with the calculated one. This is likely due to shortcomings in the [Br] parameters. In this particular case, the vdW parameters for [Br] had to be modified to fit better with the ΔH_{vap}.

Finally, Figure 12b shows results for two examples of long chain [Im$^+$]-based ILs adding evidence to our hypothesis that it is possible to transfer preparametrized functional groups to similar systems. The densities calculated for [6MIm]-based ILs show a better fit with respect to the experimental data,[57] and similar trends are observed in both cases compared to the experiment. For [6EIm], the hexyl group was transferred from [6MIm], and the imidazolium and ethyl groups were transferred from [PMIm]. In both cases, the impact of the size of the alkyl chain and the shape and size of the anion on the reproduction of bulk properties is observed again.

Enthalpy of Vaporization. The enthalpy of vaporization was calculated at the same temperatures calculated for the densities unless experimental data were available at other temperatures.

Good agreement with experimental data for [EMIm][BF_4] and [BMIm][BF_4][58] (below 10% error) is observed. As expected, the accuracy of ΔH_{vap} depends on the size of the cation and the anion (Figure 13a). This effect can be explained, at least in part, by the compensation between the Coulomb and van der Waals contributions from both types of interaction. In all cases, each methylene group was treated as an individual polarization group because it is important to account for internal polarization as discussed previously.

In the case of [BMIm][Br], [Br] vdW parameters were adjusted to improve the agreement with the experimental ΔH_{vap}.[59] Since the parameters reproduced more attractive interactions, the vdW radius of the anion was slightly increased to compensate for this contribution, which resulted in minimal impact on the density. There is evidence that ILs formed by symmetric cations of the imidazolium family present lower ΔH_{vap} than ILs composed of asymmetric cations.[60]

Figure 13b shows the predicted heats of vaporization for ILs in this study whose ΔH_{vap} has not been reported. The expected trend of lower ΔH_{vap} as the temperature rises is followed in all the examples. The enthalpy values are observed to increase as a function of the molecular weight of cations (the size of the anion is similar) as expected.

Self-Diffusion Coefficients. Self-diffusion coefficients were computed for the same three temperatures used to calculate densities in this work for IL pairs with reported experimental values. The diffusive regime was achieved by analyzing trajectories running 10 ns production after 1 ns for equilibration at the target temperature. Correction for finite-size effects were included using the correction formula by Yeh and Hummer.[44] Table 2 shows the calculated and experimental references for [EMIm] and [BMIm] (D_{cation}), both paired with [BF_4] to form the corresponding IL. The predicted D_{cation} for the rest of the ILs studied are reported in the Supporting Information.

Table 2. Comparison of Calculated and Experimental Cation Self-Diffusion Coefficient of ILs (in cm^2/s)

system	D_{cation} (exp)	D_{cation} (calc)	temperature (K)
[EMIm][BF_4]	4.2×10^{-7}	3.75×10^{-8}	293
	1.19×10^{-6}	1.10×10^{-7}	328
	2.07×10^{-6}	2.2×10^{-7}	353
[BMIm][BF_4]	2.9×10^{-7}	6.66×10^{-8}	313
	6.00×10^{-7}	1.10×10^{-7}	333
	1.1×10^{-6}	2.24×10^{-7}	353

For all the cations in this work, the calculated D_{cation} values are on the order of 10^{-8}, an order of magnitude lower than the experimental values of D_{cation}. Calculated values compared with experimental data for [EMIm][61] and [BMIm][62] are smaller. This trend is followed by all the ILs studied in this work, and it is slightly improved after using the correction formula to take into account the finite-size effect. Underestimation of self-diffusion coefficients may be due to short production times or because the parameters for ILs in this work resulted in stronger attractive interactions in the bulk between cations and anions or a combination of both. In all cases, the calculated values follow a similar expected trend to the experimental diffusion coefficients, with increasing D_{cation} as the temperature increases.

AMOEBA-IL has been shown to reproduce properties such as density within 2−5% error compared with experimental data. This is in agreement with the results reported from different force fields, polarizable and nonpolarizable.[63−65] For nonpolarizable force fields, corrections such as the scaled charge method are commonly applied to improve the performance of the force field on ionic liquid-phase properties including enthalpy of vaporization or self-diffusion coefficients. Nevertheless, this modification impacts density by systematically reducing roughly 3% the calculated values.[63]

In the case of enthalpy of vaporization property, AMOEBA-IL consistently reproduces within 12% accuracy (with the exception of [BMIm][Br]), unlike nonpolarizable force fields where errors around 30% have been reported for ionic liquids.[63,65] Site−site RDFs from AMOEBA-IL are consistent with similar interactions reported in both nonpolarizable and polarizable force fields. Low or no discrepancies were found on the peaks reported for the interactions.[63−65]

AMOEBA-IL systematically underestimates the D_{cation} by up to an order of magnitude. This trend has been reported in other scaled charge nonpolarizable force fields[65] but is improved in other polarizable force fields based on coarse-grained approach,[64] where their performance reproducing other properties such as RDF is decreased.

CONCLUSIONS

A novel method for the parametrization of imidazolium-based ILs for AMOEBA-IL has been proposed, based on the hypothesis of parameter transferability for functional groups of small molecules to bigger molecules of the same imidazolium-based family. This new parametrization procedure enables the study of 50 imidazolium-based IL pairs and provides the tools to develop transferable parameters for other cations in the future. The procedure applied to a number of ILs shows good agreement with experimental data such as density, ΔH_{vap}, and radial distribution function. Diffusion coefficients showed slower values for the calculated ILs compared with the experimental references, but similar temperature trends are

https://doi.org/10.1021/acs.jpcb.3c00986
J. Phys. Chem. B 2023, 127, 5481−5493

observed. The developed parameters have been included in the updated version of AMOEBA-IL. This procedure should be applicable to other families of cations with reasonable accuracy to ease the time for the parametrization process of new molecules included in AMOEBA-IL.

■ ASSOCIATED CONTENT

Supporting Information

The Supporting Information is available free of charge at https://pubs.acs.org/doi/10.1021/acs.jpcb.3c00986.

Plots showing the fitting from the Coulomb energy calculated with AMOEBA-IL and compared with SAPT reference; conformation analysis; densities; distribution functions diffusion results (PDF)

Computed parameters (including previously reported parameters), initial structures, additional single-molecule fitting data, and MD analysis (ZIP)

■ AUTHOR INFORMATION

Corresponding Author

G. Andrés Cisneros − *Department of Physics and Department of Chemistry and Biochemistry, University of Texas at Dallas, Richardson, Texas 75801, United States;* orcid.org/0000-0001-6629-3430; Email: andres@utdallas.edu

Author

José Enrique Vázquez-Cervantes − *Department of Chemistry, University of North Texas, Denton, Texas 76201, United States;* orcid.org/0000-0002-0127-7154

Complete contact information is available at: https://pubs.acs.org/10.1021/acs.jpcb.3c00986

Notes

The authors declare no competing financial interest.

AMOEBA-IL parameters are also available at https://github.com/TinkerTools/tinker/tree/release/params

■ ACKNOWLEDGMENTS

This work was funded by NSF Grant CHE-1856162. Computational time was provided by the University of Texas at Dallas CyberInfrastructure Facilities and the University of North Texas CASCaM CRUNTCh3 high-performance cluster supported by NSF Grants CHE-1531468 and OAC-2117247. Additional computing time from XSEDE Project TG-CHE160044 is gratefully acknowledged. The authors thank Prof. Pengyu Ren and Brandon Walker for insightful discussions. The authors thank the reviewers for insightful comments that have improved this manuscript.

■ REFERENCES

(1) Zec, N.; Vraneš, M.; Bešter-Rogač, M.; Trtić-Petrović, T.; Dimitrijević, A.; Čobanov, I.; Gadžurić, S. Influence of the Alkyl Chain Length on Densities and Volumetric Properties of 1, 3-Dialkylimidazolium Bromide Ionic Liquids and Their Aqueous Solutions. *J. Chem. Thermodyn.* **2018**, *121*, 72−78.

(2) Gupta, R.; Kartha, T. R.; Mallik, B. S. Solvation Structure and Dynamics of Alkali Metal Halides in an Ionic Liquid from Classical Molecular Dynamics Simulations. *ACS omega* **2019**, *4*, 19556−19564.

(3) Shah, F. U.; An, R.; Muhammad, N. Properties and Applications of Ionic Liquids in Energy and Environmental Science. *Front. Chem.* **2020**, *8*, DOI: 10.3389/fchem.2020.627213.

(4) Weingärtner, H. Understanding Ionic Liquids at the Molecular Level: Facts, Problems, and Controversies. *Angew. Chem., Int. Ed.* **2008**, *47*, 654−670.

(5) Plechkova, N. V.; Seddon, K. R. Applications of Ionic Liquids in the Chemical Industry. *Chem. Soc. Rev.* **2008**, *37*, 123−150.

(6) Bonhote, P.; Dias, A.-P.; Papageorgiou, N.; Kalyanasundaram, K.; Grätzel, M. Hydrophobic, Highly Conductive Ambient-temperature Molten Salts. *Inorganic chemistry* **1996**, *35*, 1168−1178.

(7) Koverga, V.; Maity, N.; Miannay, F. A.; Kalugin, O. N.; Juhasz, A.; Świątek, A.; Polok, K.; Takamuku, T.; Jedlovszky, P.; Idrissi, A. Voronoi Polyhedra as a Tool for the Characterization of Inhomogeneous Distribution in 1-Butyl-3-methylimidazolium Cation-Based Ionic Liquids. *J. Phys. Chem. B* **2020**, *124*, 10419−10434.

(8) Singh, S. K.; Savoy, A. W. Ionic Liquids Synthesis and Applications: An Overview. *J. Mol. Liq.* **2020**, *297*, 112038.

(9) Harada, L. K.; Pereira, J. F.; Campos, W. F.; Silva, E. C.; Moutinho, C. G.; Vila, M. M.; Tubino, M.; et al. Insights into Protein-ionic Liquid Interactions Aiming at Macromolecule Delivery Systems. *J. Braz. Chem. Soc.* **2018**, *29*, 1983−1998.

(10) Awad, W. H.; Gilman, J. W.; Nyden, M.; Harris, R. H., Jr; Sutto, T. E.; Callahan, J.; Trulove, P. C.; DeLong, H. C.; Fox, D. M. Thermal Degradation Studies of Alkyl-Imidazolium Salts and their Application in Nanocomposites. *Thermochim. Acta* **2004**, *409*, 3−11.

(11) Wu, J.; Yin, M.-j.; Seefeldt, K.; Dani, A.; Guterman, R.; Yuan, J.; Zhang, A. P.; Tam, H.-Y. In Situ μ-Printed Optical Fiber-Tip CO_2 Sensor Using a Photocrosslinkable Poly(ionic liquid). *Sens. Actuators, B* **2018**, *259*, 833−839.

(12) MacFarlane, D. R.; Tachikawa, N.; Forsyth, M.; Pringle, J. M.; Howlett, P. C.; Elliott, G. D.; Davis, J. H.; Watanabe, M.; Simon, P.; Angell, C. A. Energy Applications of Ionic Liquids. *Energy Environ. Sci.* **2014**, *7*, 232−250.

(13) Yeganegi, S.; Sokhanvaran, V.; Soltanabadi, A. Study of Thermodynamic Properties of Imidazolium-Based Ionic Liquids and Investigation of the Alkyl Chain Length Effect by Molecular Dynamics Simulation. *Mol. Simul.* **2013**, *39*, 1070−1078.

(14) Starovoytov, O. N.; Torabifard, H.; Cisneros, G. A. Development of AMOEBA Force Field for 1, 3-dimethylimidazolium Based Ionic Liquids. *J. Phys. Chem. B* **2014**, *118*, 7156−7166.

(15) Torabifard, H.; Reed, L.; Berry, M. T.; Hein, J. E.; Menke, E.; Cisneros, G. A. Computational and Experimental Characterization of a Pyrrolidinium-Based Ionic Liquid for Electrolyte Applications. *J. Chem. Phys.* **2017**, *147*, 161731.

(16) Bhargava, B.; Klein, M. L. Molecular Dynamics Studies of Cation Aggregation in the Room Temperature Ionic Liquid C10mim][Br] in Aqueous Solution. *J. Phys. Chem. A* **2009**, *113*, 1898−1904.

(17) Tsuzuki, S.; Shinoda, W.; Saito, H.; Mikami, M.; Tokuda, H.; Watanabe, M. Molecular Dynamics Simulations of Ionic Liquids: Cation and Anion Dependence of Self-Diffusion Coefficients of Ions. *J. Phys. Chem. B* **2009**, *113*, 10641−10649.

(18) Liu, Z.; Wu, X.; Wang, W. A Novel United-Atom Force Field for Imidazolium-Based Ionic Liquids. *Phys. Chem. Chem. Phys.* **2006**, *8*, 1096−1104.

(19) Goloviznina, K.; Canongia Lopes, J. N.; Costa Gomes, M.; Pádua, A. A. Transferable, Polarizable Force Field for Ionic Liquids. *J. Chem. Theory Comput.* **2019**, *15*, 5858−5871.

(20) Bedrov, D.; Piquemal, J.-P.; Borodin, O.; MacKerell, A. D., Jr; Roux, B.; Schröder, C. Molecular Dynamics Simulations of Ionic Liquids and Electrolytes Using Polarizable Force Fields. *Chem. Rev.* **2019**, *119*, 7940−7995.

(21) Vázquez-Montelongo, E. A.; Vázquez-Cervantes, J. E.; Cisneros, G. A. Current Status of AMOEBA-IL: A Multipolar/Polarizable Force Field for Ionic Liquids. *International Journal of Molecular Sciences* **2020**, *21*, 697.

(22) Piquemal, J.-P.; Cisneros, G. A.; Reinhardt, P.; Gresh, N.; Darden, T. A. Towards a Force Field Based on Density Fitting. *J. Chem. Phys.* **2006**, *124*, 104101.

(23) Cisneros, G. A.; Piquemal, J.-P.; Darden, T. A. Generalization of the Gaussian Electrostatic Model: Extension to Arbitrary Angular

Momentum, Distributed Multipoles, and Speedup with Reciprocal Space Methods. *J. Chem. Phys.* **2006**, *125*, 184101.
(24) Cisneros, G. A. Application of Gaussian Electrostatic Model (GEM) Distributed Multipoles in the AMOEBA Force Field. *J. Chem. Theory Comput.* **2012**, *8*, 5072−5080.
(25) Ren, P.; Ponder, J. W. Consistent Treatment of Inter-and Intramolecular Polarization in Molecular Mechanics Calculations. *Journal of computational chemistry* **2002**, *23*, 1497−1506.
(26) Ren, P.; Ponder, J. W. Polarizable Atomic Multipole Water Model for Molecular Mechanics Simulation. *J. Phys. Chem. B* **2003**, *107*, 5933−5947.
(27) Ren, P.; Wu, C.; Ponder, J. W. Polarizable Atomic Multipole-Based Molecular Mechanics for Organic Molecules. *J. Chem. Theory Comput.* **2011**, *7*, 3143−3161.
(28) Halgren, T. A. The Representation of van der Waals (vdW) Interactions in Molecular Mechanics Force Fields: Potential Form, Combination Rules, and vdW Parameters. *J. Am. Chem. Soc.* **1992**, *114*, 7827−7843.
(29) Walker, B.; Liu, C.; Wait, E.; Ren, P. Automation of AMOEBA Polarizable Force Field for Small Molecules: Poltype 2. *J. Comput. Chem.* **2022**, *43*, 1530−1542.
(30) Parrish, R. M.; Burns, L. A.; Smith, D. G.; Simmonett, A. C.; DePrince, A. E., III; Hohenstein, E. G.; Bozkaya, U.; Sokolov, A. Y.; Di Remigio, R.; Richard, R. M.; et al. Psi4 1.1: An Open-Source Electronic Structure Program Emphasizing Automation, Advanced Libraries, and Interoperability. *J. Chem. Theory Comput.* **2017**, *13*, 3185−3197.
(31) Tu, Y.-J.; Allen, M. J.; Cisneros, G. A. Simulations of the Water Exchange Dynamics of Lanthanide Ions in 1-Ethyl-3-Methylimidazolium Ethyl Sulfate ([EMIm][$EtSO_4$]) and Water. *Phys. Chem. Chem. Phys.* **2016**, *18*, 30323−30333.
(32) Tu, Y.-J.; Lin, Z.; Allen, M. J.; Cisneros, G. A. Molecular Dynamics Investigation of Water-Exchange Reactions on Lanthanide Ions in Water/1-Ethyl-3-ethylimidazolium Trifluoromethylsufate ([EMIm][OTf]). *J. Chem. Phys.* **2018**, *148*, 024503.
(33) Cisneros, G. A.; Elking, D.; Piquemal, J.-P.; Darden, T. A. Numerical Fitting of Molecular Properties to Hermite Gaussians. *J. Phys. Chem. A* **2007**, *111*, 12049−12056.
(34) Torabifard, H.; Starovoytov, O. N.; Ren, P.; Cisneros, G. A. Development of an AMOEBA Water Model Using GEM Distributed Multipoles. *Theor. Chem. Acc.* **2015**, *134*, 101.
(35) Frisch, M. J.; Trucks, G. W.; Schlegel, H. B.; Scuseria, G. E.; Robb, M. A.; Cheeseman, J. R.; Scalmani, G.; Barone, V.; Petersson, G. A.; Nakatsuji, H.; et al.*Gaussian 16*, revision C.01; Gaussian Inc: Wallingford, CT, 2016.
(36) Rackers, J. A.; Wang, Z.; Lu, C.; Laury, M. L.; Lagardère, L.; Schnieders, M. J.; Piquemal, J.-P.; Ren, P.; Ponder, J. W. Tinker 8: Software Tools for Molecular Design. *J. Chem. Theory Comput.* **2018**, *14*, 5273−5289.
(37) Darden, T.; York, D.; Pedersen, L. Particle Mesh Ewald: An Nlog(N) Method for Ewald Sums in Large Systems. *J. Chem. Phys.* **1993**, *98*, 10089−10092.
(38) Essmann, U.; Perera, L.; Berkowitz, M. L.; Darden, T.; Lee, H.; Pedersen, L. G. A Smooth Particle Mesh Ewald Method. *J. Chem. Phys.* **1995**, *103*, 8577−8593.
(39) Steinbach, P. J.; Brooks, B. R. New Spherical-cutoff Methods for Long-range Forces in Macromolecular Simulation. *J. Comput. Chem.* **1994**, *15*, 667−683.
(40) Humphrey, W.; Dalke, A.; Schulten, K. VMD − Visual Molecular Dynamics. *J. Mol. Graphics* **1996**, *14*, 33−38.
(41) Brehm, M.; Kirchner, B. TRAVIS-a Free Analyzer and Visualizer for Monte Carlo and Molecular Dynamics Trajectories. *J. Chem. Inf. Model.* **2011**, *51*, 2007.
(42) Brehm, M.; Thomas, M.; Gehrke, S.; Kirchner, B. TRAVIS—A Free Analyzer for Trajectories from Molecular Simulation. *J. Chem. Phys.* **2020**, *152*, 164105.
(43) Maginn, E. J.; Messerly, R. A.; Carlson, D. J.; Roe, D. R.; Elliot, J. R. Best Practices for Computing Transport Properties 1. Self-diffusivity and Viscosity from Equilibrium Molecular Dynamics. *Living J. Comput. Mol. Sci.* **2020**, *1*, 6324.
(44) Yeh, I.-C.; Hummer, G. System-size Dependence of Diffusion Coefficients and Viscosities from Molecular Dynamics Simulations with Periodic Boundary Conditions. *J. Phys. Chem. B* **2004**, *108*, 15873−15879.
(45) Qiao, B.; Krekeler, C.; Berger, R.; Delle Site, L.; Holm, C. Effect of Anions on Static Orientational Correlations, Hydrogen Bonds, and Dynamics in Ionic Liquids: A Simulational Study. *J. Phys. Chem. B* **2008**, *112*, 1743−1751.
(46) Xu, W.-G.; Li, L.; Ma, X.-X.; Wei, J.; Duan, W.-B.; Guan, W.; Yang, J.-Z. Density, Surface Tension, and Refractive Index of Ionic Liquids Homologue of 1-Alkyl-3-Methylimidazolium Tetrafluoroborate [$C_n$mim][BF_4](n = 2, 3, 4, 5, 6). *Journal of Chemical & Engineering Data* **2012**, *57*, 2177−2184.
(47) Shamsipur, M.; Beigi, A. A. M.; Teymouri, M.; Pourmortazavi, S. M.; Irandoust, M. Physical and Electrochemical Properties of Ionic Liquids 1-ethyl-3-methylimidazolium tetrafluoroborate, 1-butyl-3-methylimidazolium trifluoromethanesulfonate and 1-butyl-1-methyl-pyrrolidinium bis (trifluoromethylsulfonyl) imide. *J. Mol. Liq.* **2010**, *157*, 43−50.
(48) Paulechka, Y. U.; Kabo, A. G.; Blokhin, A. V.; Kabo, G. J.; Shevelyova, M. P. Heat Capacity of Ionic Liquids: Experimental Determination and Correlations with Molar Volume. *Journal of Chemical & Engineering Data* **2010**, *55*, 2719−2724.
(49) Song, D.; Chen, J. Density and Viscosity Data for Mixtures of Ionic Liquids with a Common Anion. *Journal of Chemical & Engineering Data* **2014**, *59*, 257−262.
(50) Součková, M.; Klomfar, J.; Pátek, J. Surface Tension and 0.1 MPa Density of 1-Alkyl-3-Methylimidazolium Tetrafluoroborates in a Homologous Series Perspective. *J. Chem. Thermodyn.* **2016**, *100*, 79−88.
(51) Součková, M.; Klomfar, J.; Pátek, J. Group Contribution and Parachor Analysis of Experimental Data on Density and Surface Tension for Members of the Homologous Series of 1-Cn-3-Methylimidazolium Chlorides. *Fluid Phase Equilib.* **2017**, *454*, 43−56.
(52) Kumar, A. Estimates of Internal pressure and Molar Refraction of Imidazolium Based Ionic Liquids as a Function of Temperature. *J. Solution Chem.* **2008**, *37*, 203−214.
(53) Zhou, Q.; Wang, L.-S.; Chen, H.-P. Densities and Viscosities of 1-Butyl-3-Methylimidazolium Tetrafluoroborate + H_2O Binary Mixtures from (303.15 to 353.15) K. *Journal of Chemical & Engineering Data* **2006**, *51*, 905−908.
(54) Klomfar, J.; Součková, M.; Pátek, J. Experimental Densities and Surface Tension and Models Generating the Best-Current-Knowledge Values of them for Members of 1-Cn-3-Methylimidazolium Bromide Homologous Series. *J. Chem. Thermodyn.* **2018**, *118*, 225−234.
(55) Kim, K.-S.; Shin, B.-K.; Lee, H. Physical and Electrochemical Properties of 1-Butyl-3-Methylimidazolium Bromide, 1-Butyl-3-Methylimidazolium Iodide, and 1-Butyl-3-Methylimidazolium Tetrafluoroborate. *Korean Journal of Chemical Engineering* **2004**, *21*, 1010−1014.
(56) Pal, A.; Kumar, B.; Kang, T. S. Effect of Structural Alteration of Ionic Liquid on their Bulk and Molecular Level Interactions with Ethylene Glycol. *Fluid Phase Equilib.* **2013**, *358*, 241−249.
(57) Mac Dowell, N.; Llovell, F.; Sun, N.; Hallett, J.; George, A.; Hunt, P.; Welton, T.; Simmons, B.; Vega, L. New Experimental Density Data and Soft-SAFT Models of Alkylimidazolium ([C n C1im]+) Chloride (Cl−), Methylsulfate ([$MeSO_4$]-), and Dimethylphosphate ([Me2PO_4]-) Based Ionic Liquids. *J. Phys. Chem. B* **2014**, *118*, 6206−6221.
(58) Deyko, A.; Lovelock, K. R.; Corfield, J.-A.; Taylor, A. W.; Gooden, P. N.; Villar-Garcia, I. J.; Licence, P.; Jones, R. G.; Krasovskiy, V. G.; Chernikova, E. A.; et al. Measuring and Predicting Δ vap H 298 Values of Ionic Liquids. *Phys. Chem. Chem. Phys.* **2009**, *11*, 8544−8555.
(59) Verevkin, S. P.; Emel'yanenko, V. N.; Zaitsau, D. H.; Ralys, R. V.; Schick, C. Ionic Liquids: Differential Scanning Calorimetry as a

https://doi.org/10.1021/acs.jpcb.3c00986
J. Phys. Chem. B 2023, 127, 5481−5493

New Indirect Method for Determination of Vaporization Enthalpies. *J. Phys. Chem. B* **2012**, *116*, 4276−4285.
(60) Yermalayeu, A. V.; Zaitsau, D. H.; Loor, M.; Schaumann, J.; Emel'yanenko, V. N.; Schulz, S.; Verevkin, S. P. Imidazolium Based Ionic Liquids: Impact of the Cation Symmetry and Alkyl Chain Length on the Enthalpy of Vaporization. *Zeitschrift für anorganische und allgemeine Chemie* **2017**, *643*, 81−86.
(61) Noda, A.; Hayamizu, K.; Watanabe, M. Pulsed-Gradient Spin-Echo 1H and 19F NMR Ionic Diffusion Coefficient, Viscosity, and Ionic Conductivity of Non-Chloroaluminate Room-Temperature Ionic Liquids. *J. Phys. Chem. B* **2001**, *105*, 4603−4610.
(62) Tokuda, H.; Tsuzuki, S.; Susan, M. A. B. H.; Hayamizu, K.; Watanabe, M. How Ionic are Room-Temperature Ionic Liquids? An Indicator of the Physicochemical Properties. *J. Phys. Chem. B* **2006**, *110*, 19593−19600.
(63) Doherty, B.; Zhong, X.; Gathiaka, S.; Li, B.; Acevedo, O. Revisiting OPLS Force Field Parameters for Ionic Liquid Simulations. *J. Chem. Theory Comput.* **2017**, *13*, 6131−6145.
(64) Uhlig, F.; Zeman, J.; Smiatek, J.; Holm, C. First-Principles Parametrization of Polarizable Coarse-Grained Force Fields for Ionic Liquids. *J. Chem. Theory Comput.* **2018**, *14*, 1471−1486.
(65) Goloviznina, K.; Canongia Lopes, J. N.; Costa Gomes, M.; Pádua, A. A. Transferable, Polarizable Force Field for Ionic Liquids. *J. Chem. Theory Comput.* **2019**, *15*, 5858−5871.

https://doi.org/10.1021/acs.jpcb.3c00986
J. Phys. Chem. B 2023, 127, 5481−5493